JOINT INSTITUTE FOR NUCLEAR RESEARCH

2010-14

E. A. Krasavin, G. N. Timoshenko

LABORATORY OF RADIATION BIOLOGY RESEARCH ACTIVITIES IN 2003–2009

Report to the 107th Session
of the JINR Scientific Council
February 18–19, 2010

Dubna 2010

E. A. Krasavin, G. N. Timoshenko

LABORATORY OF RADIATION BIOLOGY RESEARCH ACTIVITIES IN 2003–2009

Report to the 107th Session
of the JINR Scientific Council
February 18–19, 2010

Dubna 2010

1. Scientific research programme for 2009

In 2009, the research programme of the Laboratory of Radiation Biology (LRB) determined by 1st priority theme 04-9-1077-2009/2011 was mainly focused in the following areas: fundamental radiobiological and radiation genetic research with heavy charged particle beams; research on the effects of accelerated heavy charged particles on eye structures (the lens and retina); molecular dynamics research; mathematical modelling of induced mutagenesis in bacterial cells; radiation research and radiation protection at JINR's basic nuclear facilities and environment. This report presents the LRB research activities during past several years.

2. Execution of the 2003–2009 programme

2.1. Radiobiological and radiation genetic research

Molecular radiobiology

A large cycle of research on the regularities and mechanisms of the genetic effect of radiations in a wide range of linear energy transfer (LET) carried out. Using heavy ion beams of JINR's accelerators, it was established that the effectiveness of heavy charged particles on the genetic structures of cells with different genotype evaluated against different criteria (the lethal effect, gene and deletion mutation induction, transposon excision, formation of DNA double-strand breaks (DSBs)) is determined by the specifics of the radiation energy microdistribution in the genetic structures influencing the character of the induced DNA lesions and by the efficiency of the cell repair systems working towards repairing the damaged structures. It was shown that the regularities and mechanisms of the gene and deletion mutation induction in bacteria by radiations with different physical characteristics are different. The quadratic component of the dose dependence of the frequency of the gene mutations that are formed with the participation of the inducible, error-prone branch of SOS repair is present under all used radiations. The deletion mutation induction frequency is linearly related to the dose of the irradiation of cells by γ-quanta and heavy charged particles. The differences in the character of the dose dependences of mutagenesis in the radiation-induced gene and deletion mutations are caused by different types of DNA lesions involved in the mutation process (clustered single-strand breaks of DNA during the formation of gene mutations and DNA DSBs during the

formation of deletions) and by different repair mechanisms participating in induced mutagenesis.

It was established that precise transposon excision induced by radiations with different physical characteristics, being a deletion process by its molecular nature, depends on the level of the expression of the genes regulating SOS repair (Fig. 1). The determinancy of the precise transposon excision by the inducible SOS repair system and the power character of the dose dependence of this process under γ-quanta and charged particles are conditioned by the induction of DNA lesions that are close to each other in terms of their molecular nature and participate in the formation of the gene mutations and precise transposon excision.

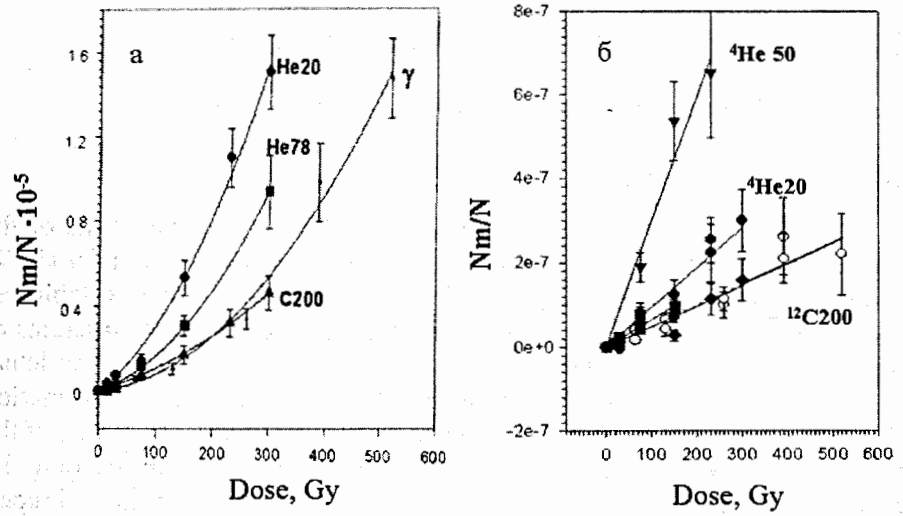

Fig. 1. The frequency of gene (a) and structural (b) mutation induction in *Escherichia coli* bacteria by accelerated heavy ions. He20, He78, and C200 denote ion types and their LET, keV/μm.

The relative biological effectiveness (RBE) of accelerated heavy ions, which was studied in terms of different aspects of radiation action (the lethal effect, gene and deletion mutation induction, precise transposon excision, and the formation of DNA DSBs), depends on LET of heavy particles. It was shown that with an increase in LET, the RBE coefficients of heavy ions estimated on the basis of their lethal action, gene and deletion mutation induction, and precise transposon excision increase (Fig. 2). The LET value, to which maximal RBE coefficients correspond (L_{max}), varies depending on the character of the observed radiation-induced effect: for the gene

mutations and precise transposon excision, the L_{max} values are found in the range of LET that is much lower than for the lethal effect and deletion mutation induction. For the studied radiation-induced effects, the differences in the L_{max} location are determined by different types of DNA lesions involved in the mutation process.

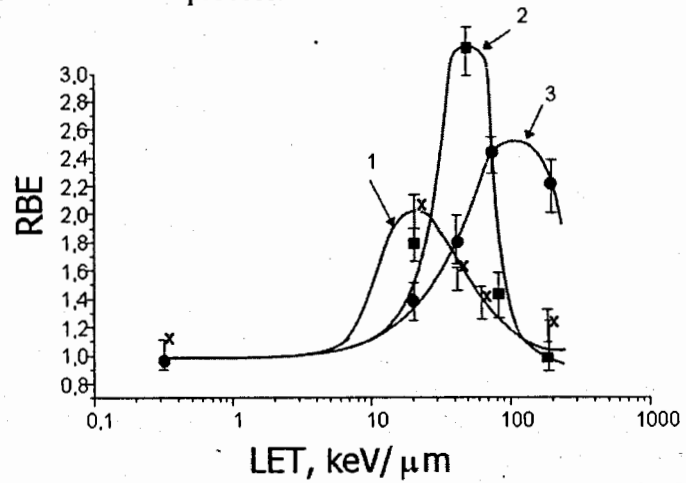

Fig. 2. RBE dependence on LET against the following criteria: gene mutation induction (1), deletion induction (2), and lethal effect of radiations (3).

As is known, DNA DSBs underlie the structural disorders in genetic material. They lead to the formation of structural mutations in genes, chromosome aberrations, cell transformation initiation, and programmed cell death (apoptosis). It was shown that the character of the DNA lesions formed under heavy charged particles significantly differs from that of the γ-induced lesions. Contrary to γ-quanta, accelerated heavy ions initiate mainly cluster-type lesions in DNA [Michalik, 1992, Chatterje and Holley, 1993]. A cluster lesion is a combination of instantaneous lesions in a DNA part followed by the formation of single-strand breaks, modification of bases, and modification of sugar. The events of this kind result from a local deposition of a great amount of energy as a heavy charged particle passes through a DNA strand.

In experiments on human lymphocytes using the DNA comet method, it was shown that high-energy carbon ions initiate DNA DSBs with an efficiency compared with that of γ-quanta (Fig. 3). The kinetics of DNA DSB repair under high-energy heavy charged particles is comparable with that of γ-irradiation. The low biological effectiveness of this type of radiation is determined by low LET levels of high-energy carbon ions.

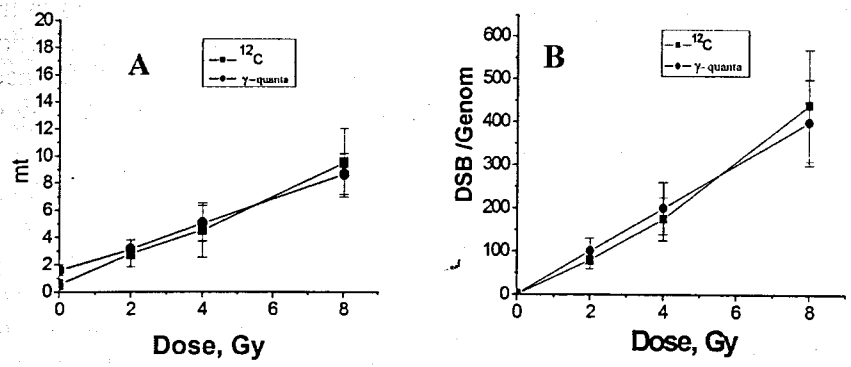

Fig. 3. DNA DSB induction in human lymphocytes by irradiation with ^{60}Co γ-rays and accelerated carbon ions with an energy of 480 MeV/nucleon: the dependence of the parameter mt (comet tail moment) on the irradiation dose (A); the dependence of the DNA DSB number per genome on the irradiation dose (B).

Using the comet analysis method, regularities were studied in the formation and repair of DNA DSBs under irradiation with ^{60}Co γ-quanta, ^{11}B ions with a LET of 40 keV/μm, and ^{7}Li ions with a LET of 20 keV/μm (Fig. 4). Cell distributions over the damage level upon irradiation with γ-quanta and heavy ions were obtained. It was shown that the biological effectiveness of heavy ions based on the DNA DSB induction criteria is higher than that of γ-radiation. As can be seen in Fig. 4, the obtained dose dependences of DNA DSB induction by γ-quanta, ^{11}B ions, and ^{7}Li ions are linear. The RBE values of accelerated B and Li ions are 1.7 ± 0.1 and 1.6±0.1, respectively.

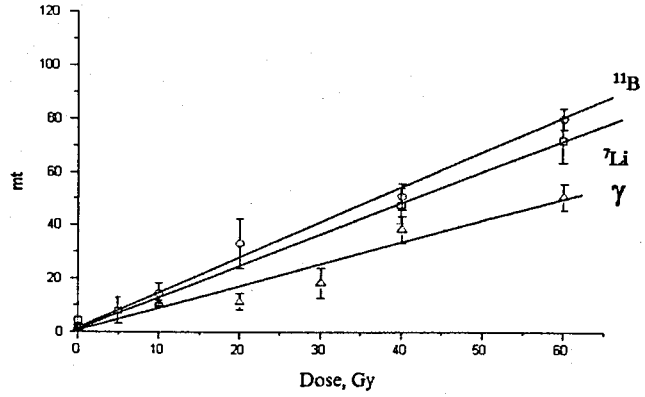

Fig. 4. The dose dependence of DNA DSB induction in human lymphocytes by γ-quanta, accelerated boron ions with a LET of 40 keV/μm, and accelerated lithium ions with a LET of 20 keV/μm.

Regularities in DNA DSB formation in human lymphocytes were studied in different cell cycle phases (G_0, S, G_1 and G_2) after irradiation with ^{60}Co γ-quanta and 250-MeV Bragg peak protons (Fig. 5). The maximal DNA DSB yield was observed in the S phase of the cell cycle. The kinetics of DNA DSB repair in lymphocytes stimulated by phytohemagglutinin was studied at different times after irradiation (24, 48, 72, and 96 hours). It was found that DNA DSB yield decreases exponentially during the post-irradiation period. The reference level of DNA DSBs was observed 24 h after irradiation, which remained so until 96 h.

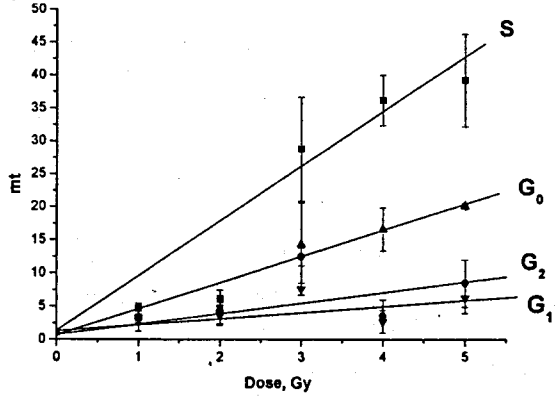

Fig. 5. DNA DSB induction in human lymphocytes in different cell cycle phases after irradiation with Bragg peak protons.

Regularities were studied in DNA DSB induction and repair under γ- and ^{11}B ion (40 keV/μm) irradiation in the presence of DNA synthesis inhibitors: cytosine arabinoside (Ara-C) and hydroxyurea (HU). A combination of these agents blocks both replicative and reparative synthesis of DNA. In these conditions, the radiation-induced short single-strand gaps in DNA transform into double-strand enzymatic breaks because the strands that are opposite to the gap had been attacked by S_1 endonucleases, which are specific to the single-strand DNA. It was shown that the blocking of the reparative synthesis of DNA leads to an increase in DSB yield during the post-irradiation period.

Using a DNA comet method, a comparative analysis was performed of regularities in the induction and repair of DNA single- and double-strand breaks (SSBs and DSBs, respectively) in human lymphocytes under ^{60}Co γ-irradiation. It is shown that the dependence of DNA SSB and DSB yield increases linearly with the irradiation dose, DNA SSB formation efficiency being substantially higher. The kinetics of DNA SSB and DSB repair in

lymphocytes after γ-irradiation was studied. It was found that DNA SSB and DSB yield decreases exponentially during the post-irradiation period.

Using a morphological method involving fluorescent staining of samples by a mixture of dyes (ethidium bromide and acridine orange), regularities were studied in the induction of apoptosis by ^{60}Co γ-quanta in human lymphocytes at different times after irradiation: 0, 24, 48, and 72 hours. Variability of the results was observed between donors of different ages (21– 62 years).

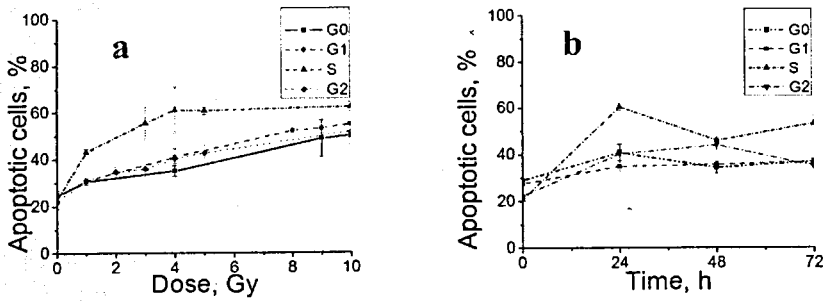

Fig. 6. a) Apoptosis induction in human lymphocytes in different cell cycle phases.
b) Apoptosis kinetics in different cell cycle phases.

Regularities were studied in the induction of apoptosis in human lymphocytes in different phases of the cell cycle after irradiation with γ-quanta and Bragg peak protons (Fig. 6). It was shown that cells in the G_2 and S phases are the most sensitive against this criterion.

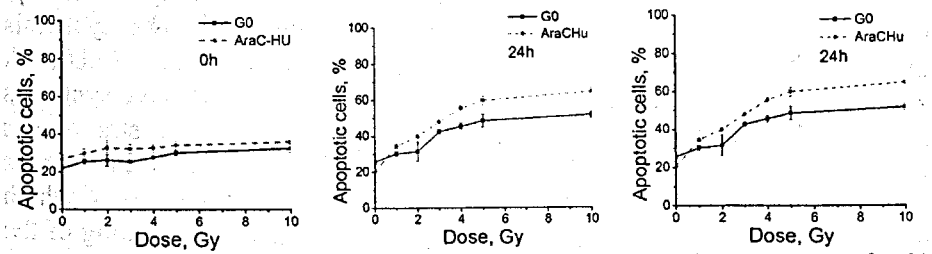

Fig. 7. Apoptotic cell induction after γ-irradiation of lymphocytes in the presence of DNA repair inhibitors Ara-C and HU after 0 h (left), 24 h (middle), and 48 h (right).

The influence of inhibitors of the replicative and reparative DNA synthesis – cytosine arabinoside (Ara-C) and hydroxyurea (HU) – on the kinetics of γ-induced apoptosis in human lymphocytes was studied. It was shown that in the presence of inhibitors, the induced apoptosis frequency increases, which correlates with the active accumulation of enzymatic DNA

DSBs in these conditions. As is known, DSBs are the molecular basis of the events triggering apoptosis (Fig. 7).

The influence of the combined effect of γ-radiation and lipid *A* obtained from *Escherichia coli* on the phagocyte, lysozyme, and peroxidase activities of human leukocytes was studied. It was found that a low concentration of lipid *A* significantly influences human cells under γ-irradiation by increasing their phagocyte and lysozyme activity. Besides, under low doses of irradiation, lipid *A* decreases peroxidase activity. On the grounds of the obtained results, a conclusion was made that under ionizing radiation lipid *A* has a modifying effect on the phagocyte, lysozyme, and peroxidase properties of the cells forming immune response.

Taking into account the performed work, further research on the genetic effect of high-energy heavy charged particles is planned, which will facilitate the solution of many practical issues challenging space radiobiology, radiation genetics, and medicine.

Radiation genetics of lower eukaryotes

In 2009, research was continued on the regularities in the mutation process in Saccharomycetes. Regularities were studied in the occurrence of spontaneous mutations and mutations induced by electromagnetic radiation (ultraviolet light) and ionizing radiation (γ-rays) depending on the checkpoint control functionality and the mitochondrial activity. In this work, genetic systems were used to test recombination (interchromosomal and intrachromosomal recombination, including recombination accompanied by the formation of deletions), deletions, and frame shift mutations. To suppress checkpoint control, mutants of the *rad53* kinase, which participates in the activation of numerous ways of checkpoint control, were used. Experiments showed that the *rad53* mutation suppresses deletion mutagenesis, and the *RAD53* gene participates in the NHEJ accompanied by the formation of deletions. Besides, the influence of the mitochondrial functionality on the level of mutagenesis was studied. The respiration activity in mitochondria was suppressed in experiments by the rho$^-$ and rho^0 mutations of respiratory failure. It was shown that respiratory disorder influences the survival rate, recombination, and formation of deletions, while no influence on the formation of the frame shift mutations was observed.

Research was started on the participation of mutations localized in the genes coding the subunits of protein complexes (e.g. the CDC28 kinase,

SAGA histoneacetyltransferase, and regulator of the Sir2 deacetylase localization) in cell apoptosis and ageing. It was shown earlier by the Radiation Genetics of Yeasts research group that these genes participate in repair and checkpoint control.

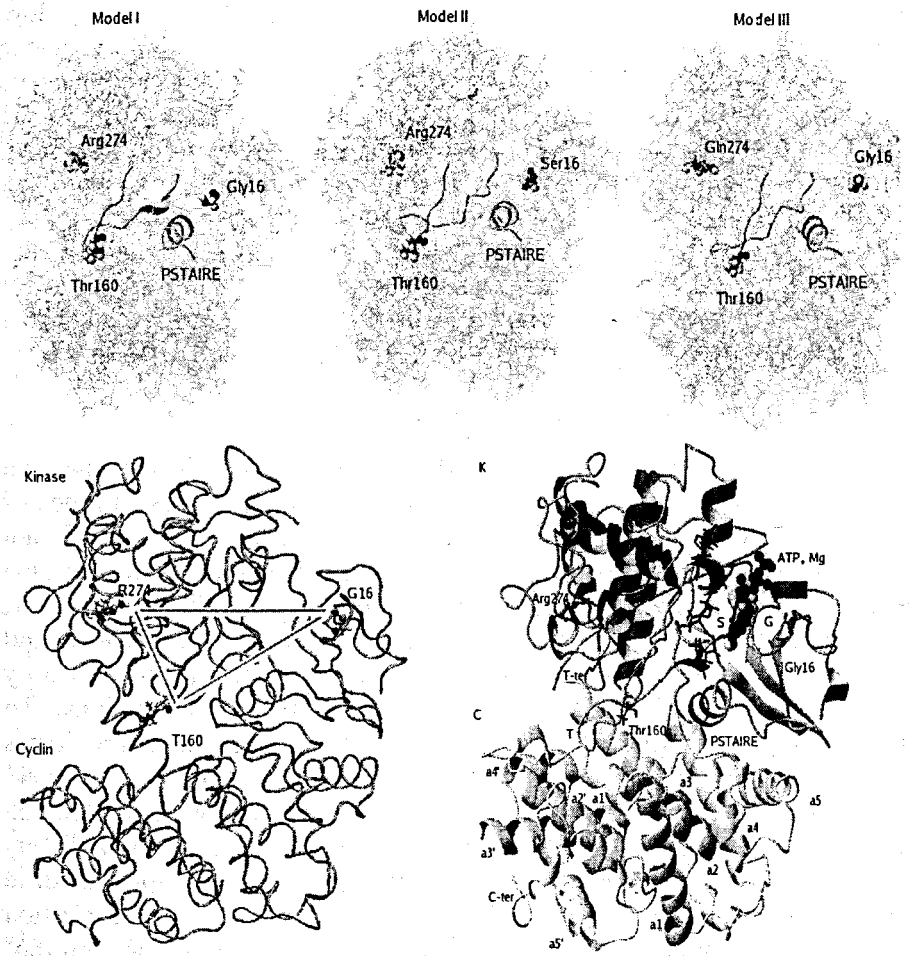

Fig. 8. A model of the CDK2 kinase and cyclin A. The positions of the studied amino acid residues G16 in the G loop of the small lobe, R274 in the large lobe, and T160 in the T loop of the large lobe of the kinase are shown.

The CDC28 kinase plays a key role in the cell cycle regulation. Studies of the pleiotropic manifestations of the *cdc28-srm* [Gly20Ser] mutation and the *cdc28-13* [Arg283Gln] mutation is topical because

disorder in the functioning of the homologous kinase in human cells leads to the malignant transformation of cells.

The use of dynamic modeling allowed the determination of the structure changes induced by the corresponding mutations in the homologous human CDK2 kinase. The *cdc28-srm* mutation consists in a substitution for the third glycine in the GxGxxG conservative sequence in the so called G-rich loop in the small lobe of the kinase subunit; it is located against the T loop in the large lobe of the kinase subunit. Although the importance of the G and T loops is established, their role is still poorly studied. To investigate the structure of kinases, including CDC28, the crystal structure of the human CDK2 kinase is used now. The analysis of the nanosecond dynamics of the CDK2/ATP complex progression has been continued. The molecular dynamics modeling of the mutant structures of the kinase with substitutions for the CDK2-G16S amino acid in the G-rich loop of the small lobe and CDK2-R284Q amino acid in the large lobe showed the importance of these amino acids and their influence on the CDK2 kinase conformation, which is observed as an increase in the distance between the G and T loops in the corresponding mutant forms. The obtained results show that mutations destabilize the local structure in the T loop area (Fig. 8). The Arg284→Gln284 mutation in the distant C-end area has a more pronounced effect and leads to the loosening of the kinase structure and an increase in the distance between the G and T loops. Research on the tertiary structure of the native and mutant proteins is promising for the development of medicines.

Radiation cytogenetics

The main aim of the research performed by the Radiation Cytogenetic Group was to assess the variability of individual sensitivity to high-LET radiation. For this purpose, aberrations induced in the G0 and G2 cell cycle stages in human blood lymphocytes irradiated with γ-rays and charged particles of different LET were analyzed. Whole blood samples were irradiated with γ-rays (4 donors), protons (7 donors), ^{12}C (9 donors), ^{7}Li (2 donors), ^{11}B (3 donors, and ^{20}Ne ions (4 donors). The ion beam energies and LET values were, respectively, as follows: protons – 170 MeV and ≈ 0.5 keV/μm; ^{12}C – 480 MeV/amu and 10.6 keV/μm; ^{7}Li – 30 MeV/amu and 20 keV/μm; ^{11}B – 32 MeV/amu and 55 keV/μm; ^{20}Ne –53 MeV/amu and 170 keV/μm. Chromosome aberrations induced in the G0 and chromatid aberrations induced in the G2 cell cycle stages were measured both with

conventional metaphase technique (in normal mitotic cells) and with the premature chromosome condensation (PCC) technique (calyculin A-induced premature chromosome condensation). For chromosome aberration analysis, lymphocytes exposed to protons, ^{7}Li, ^{11}B, and ^{20}Ne ions were harvested at several sampling times (48 – 70 h). A fluorescent in situ hybridization (FISH) analysis of stable and unstable chromosome aberrations was performed in prematurely condensed chromosomes of peripheral blood lymphocytes (PBL) exposed to protons, ^{12}C, ^{7}Li, and ^{11}B and incubated for 48 h.

A clear inter-individual variability was observed for both chromosome and chromatid aberration yields. Generally, the results show a greater inter-donor variability of aberration frequencies for charged particles than for γ-rays. Some disagreement concerning the level of radiosensitivity was seen between conventional metaphase analysis and the PCC method. To compare the variability in aberration frequencies induced by different radiation types, the coefficient of variability was calculated for both chromosome and chromatid aberrations. On the average, the frequencies of aberrations induced in G2 show a greater interdonor variability than those induced in G0.

Also, aberrations scored by conventional Giemsa method and PCC+FISH were used for the assessment of the interindividual variability of the F (the ratio of dicentric to ring frequencies) and C (the ratio of complex to simple aberrations frequencies) ratios in chromosomes of peripheral blood lymphocytes from several donors irradiated by protons and heavy ions of different LET. The F ratio was found to be dose dependent for γ-rays, whereas no dependence was seen for dose and sampling time for charged particles. Results of the PCC+FISH analysis show a considerably higher F ratio for protons than for heavier ions. On the average, the C ratio was found to be corresponding to LET. The inter-donor variability of the C ratio was greater than that of the F ratio. These results explain very well the difference between data obtained at other laboratories over the world and confirm the importance of PCC+FISH analysis for determining the quality of radiation in biological dosimetry.

In 2009, the study of the chromosome aberrations in human blood lymphocytes irradiated with protons at the therapeutic beam of the JINR Phasotron in different cell cycle phases won the second prize for research and applied work of the 13th conference of JINR's Association of Young Scientists and Specialists.

Radiobiology of normal and tumor cells

It was previously shown that low dose γ-irradiation induces complex nonlinear dependences of the number of aberrant cells on the dose. The region of high sensitivity to chromosome damage has been identified in mammalian cells at doses below 5–7 cGy, which precedes the occurrence of increased radioresistance (IRR). The nature of these phenomena is unknown. We have assumed that observed hyperradiosensitivity (HRS) could be a consequence of radiation-induced increase of reactive oxygen species (ROS) production in normal metabolism. This occurs, in particular, in the mitochondrial electron transport chain due to mitochondrial permeability transition (MPT). On the other hand, radiation-induced amplification of ROS was shown to be a sensing mechanism for activation of cellular cytoprotective pathways. Extracellular signal-regulated kinase ERK seemed to be more appropriate as a candidate for the main protective protein in this case. Based on these findings, it was suggested that the activation of pathways aimed at reducing oxidative stress may cause a decrease in the number of aberrant cells observed in experiments after HRS. To investigate this hypothesis, it was examined whether substances affecting ROS, MPT and ERK-activity would prevent arising HRS and IRR modifying as a result of the dose–effect shape.

Human mammary carcinoma cells cal51 were exposed to1–20 cGy γ-irradiation in the presence of different modifiers: an activator of ERK – TPA, inhibitor of ERK – PD98059 and inhibitor of MPT – CsA; the ROS-scavenger DMSO was added immediately after irradiation so as not to affect radicals appearing due to water radiolysis. The number of aberrant anaphases was assessed after 8-hours incubation. The results are presented in the Fig. 9.

DMSO prevents both HRS and IRR bringing the shape of dose-response curve closer to linear. The effect of the CsA is more pronounced: the aberrant cells yield drops to nearly the background level in the presence of this drug. There is a significant decrease in the number of aberrant cells treated with the ERK-activator. This is most dramatic in the region of HRS. Conversely, the cells pretreated with the ERK-inhibitor lose IRR observed in untreated samples.

These results strongly point ROS being the mediator of hyperradiosensitivity at low doses as well as signaling molecules of cytoprotective mechanism activation. As CsA-treatment shows these ROS

are mitochondrial in origin. Activation of ERK is required to protect cells against oxidative damage caused by ROS.

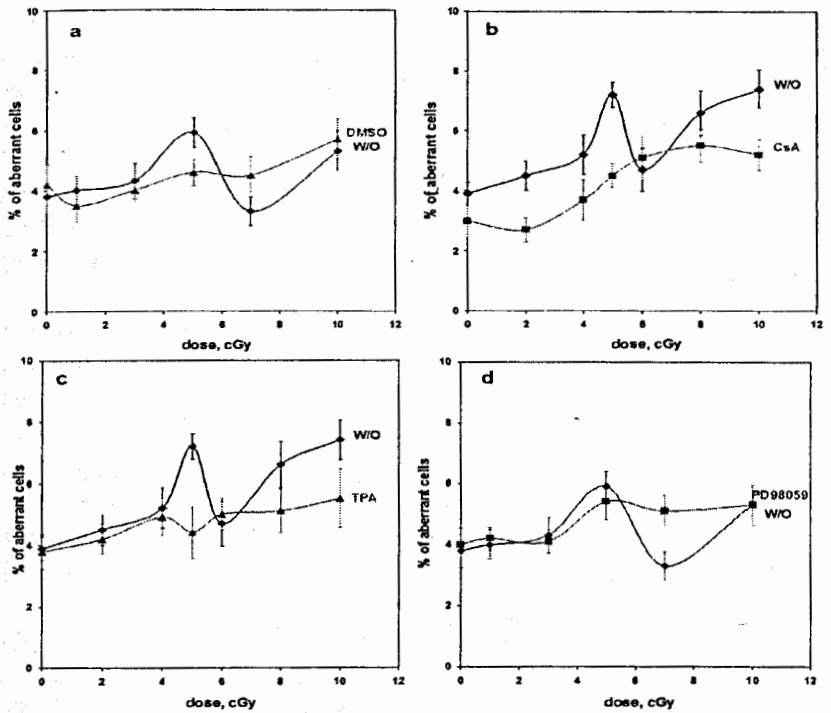

Fig. 9. Effect of modifiers on the frequency of aberrant cells induced by low dose γ-irradiation in mammary carcinoma cells cal51.

The investigation of adaptive response (AR) was continued on human lymphocytes. AR is the phenomenon by which cells exposed to low dose of radiation become less sensitive to subsequent high-dose exposure. It is assumed that AR could be a consequence of IRR as a result of protective mechanisms induction. No clear correlation between these phenomena was established due to high intra- and inter-donor variability.

Mathematical simulation of radiation-induced mutagenesis

New mathematical approaches to the modeling of the mutation process induced by ultraviolet (UV) radiation in *Escherichia coli (E. coli)* bacterial cells were developed. A model was proposed that presents the induced mutation process in terms of a detailed mathematical description of the key protein interactions in the course of the functioning of the *E. coli*

SOS response system. For the first time, a connection is shown between the SOS response processes and translesion synthesis (TLS) efficiency; the whole chain of events from a damaging factor affecting the cell to the mutation formation in the DNA chain is analyzed in detail. Numerical solutions of the model's equations for each protein of the SOS system were obtained.

A mathematical model of TLS in *E. coli* bacterial cells was developed. A quantitative evaluation was performed of the probability of the occurrence of a certain number of errors during TLS. On the basis of the proposed model concepts, a quantitative estimation was performed of the gene mutation yield under UV irradiation. Using the *lacI* regulatory gene of *E. coli*, the dependence was calculated of the mutation frequency on the UV dose. For specific values of the model's free parameters, the modeling results match the experimental data.

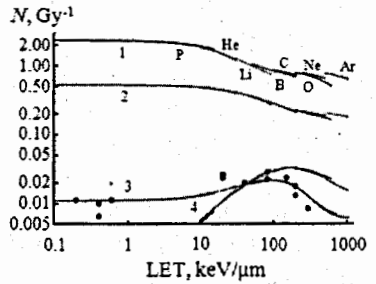

Fig. 10. The yield per one genome of base lesions (1), DNA single-strand breaks (2), clustered lesions (3), and DNA double-strand breaks (4) depending on the LET of particles with an energy of 3–10 MeV/nucleon. (dots are the experimental data characterizing the dependence of the quantity SOSIP on the LET of radiations).

A mathematical model was developed that describes the dynamics of the inducing signal of the SOS system in *E. coli* bacterial cells under accelerated ions. Using the earlier developed model, the process of the formation of the main pre-mutation DNA lesions – base lesions (BL), single- and double-strand breaks (SSB and DSB), and clustered lesions (CL) – was described. In the used model, DNA is considered to be a linear target randomly positioned relative to the charged particle track. The proposed model takes into account the radial energy distribution in the particle tracks, which is very important for the assessment of the role of the delta electrons in the radiobiological effects of radiations with different LET.

Fig. 10 shows the comparative calculation of the BL, SSB, DSB, and CL yield depending on LET of different types of ions. The obtained results

confirm that the character of the BL yield dependence on LET is similar to that of the DNA SSB yield dependence on LET, the DNA BL yield being four times higher than the SSB yield over the whole measured LET range due to an effective increase in the thickness of the linear DNA target. The DSB and CL yields are described by a curve with a maximum, after which any further increase in LET is inefficient. A comparison was made between the calculation results describing the total yield of CL (independently of their type) and experimental data characterizing the dependence of the quantity SOS induction potency (SOSIP) measured by the SOS chromotest method on LET of radiations. The calculation results were found to agree with the experimental data

Models were developed of the main types of repair which lead to the formation of an inducing signal for the SOS system. It is the presence of single-strand parts of DNA that is the signal. As part of the research, the following types of repair were modeled: SSB repair involving DNA polymerase I, DSB repair by homologous recombination, modified base reconstruction by excision repair, and clustered lesion repair by SOS response. The models take into account the processes of clustered lesions transforming into DSBs and the transformation of DSBs into SSBs with the development of a temporary or permanent heteroduplex.

Results were obtained that characterize the inducing signal concentration dynamics under the influence of different types of ions in wild-type *E. coli* cells and in *umuDC* mutants.

A stochastic SOS response model was developed based on the Gillespie algorithm, which is widely used to model complex biological systems. This approach has the advantages of the correct description of the kinetics of the main protein interactions during SOS response in an isolated bacterial cell under low energy fluences of ultraviolet (UV) radiation (<1 J/m^2), and a possibility of the quantitative evaluation of the survival rate of cells under UV radiation. The proposed model allows the description of SOS response kinetics in *E. coli* bacterial cells for an arbitrary value of the energy fluence of UV radiation and, in perspective, can be extended to include other external damaging factors. In this work, the dynamics of primary and secondary DNA lesion formation and the main protein complexes in an isolated cell, and the survival rate of a cell population were calculated. Significant fluctuations of the concentration of the SOS system proteins were revealed in the case of a small number of molecules for the dimerized products of the *umuD* gene.

2.2. *Photoradiobiological research*

A cataract, which is an opacity of the lens, is one of the main causes of eyesight deterioration. The initiation and development of a cataract is a disease that goes along with aging; moreover, it can be a marker of the organism aging. A lot of internal and external factors accelerate cataract development. For example, an increase in the blood sugar level makes for the diabetic cataract; ultraviolet (UV) irradiation leads to the UV cataract. A hypothesis has been around for more than 50 years that radiation accelerates aging. From this viewpoint, a radiation cataract can be considered to be a senile one. The lens opacity associated with a radiation cataract has a local character. In recent years, however, evidence appeared that cosmonauts' cataract has a diffuse character. In this connection, it was suggested that this kind of cataract can be caused by the specifics of galactic radiation, which includes heavy charged particles (HCP). HCP damage crystallins (the lens proteins) causing internal breaks in molecules. After returning to the Earth, the lens is exposed to UV radiation, which reveals these "weakened" molecules; then the protein is denatured and aggregated. The short-range packing of molecules is thus disordered; local changes in protein concentration appear; and, as a result, the medium refraction coefficient locally changes; light scattering is enhanced; and an opacity develops.

To check this hypothesis, two series of experiments were performed: an *in vitro* study of HCP irradiation of crystallin solutions aimed at determining changes in their stability, and an *in vivo* study of cataract induction by radiation combined with UV rays.

- *An in vitro study of changes in the stability of solutions of crystallins under* HCP *irradiation*

Solutions of the α and β_L crystallins of a bull lens obtained by gel filtration were irradiated by B^{11}, C^{12} and Li nuclei; then, structural and functional changes in the proteins were studied. The research focused on the stability of the β_L crystallin against heating- and photo-induced denaturation, as well as the chaperone activity of the α crystallin against the heating- and photo-induced denaturation of the β_L crystallin. The structural changes in the proteins were characterized using tryptophan and non-tryptophan fluorescence techniques, gel filtration, and electrophoresis in polyacrylamide gel (PAAG) in denaturating and reducing conditions. Irradiation with 32-MeV B^{11} nuclei did not lead to any evident changes in the stability of the β_L crystallin against thermal denaturation, while a dose of

8 Gy resulted in a 30% shortening of the photo aggregation lag period under UV light. The electrophoresis data showed no irradiation-induced changes in the polypeptide composition of the samples. A study of fluorescence spectra indicates that there are certain conformational restructurings in the β_L crystallin molecule already at a dose of 4 Gy.

- *Cataract induction by γ-radiation combined with UV radiation*

Four randomized groups of F1 male mice (C57Black/CBA) were daily exposed to whole-body UV-irradiation (280–380 nm, 15 min, 5.5±0.8 W/m^2); once – to a whole-body γ-irradiation with a dose of 2 Gy; and to a combination of these factors (γ and UV rays). Group 4 was used as the reference for the age-related changes (R). The development of a cataract in the 7th and 10th months was evaluated by the peer review method using a 6-point scale. In the 7th month, the lens opacity was as follows. R: 0.0; UV: 2.50 ± 0.13; γ-rays: 1.00 ± 0.28; γ-rays+UV: 4.00 ± 0.45 (median±σ). The differences between the groups are reliable ($p<0.001$ against the Mann – Whitney U-test). In the 10th month, the lens opacity significantly increased; its values were the following. R: 2.75 ± 0.17; UV: 5.75 ± 0.42; γ-rays: 6.00 ± 0.29; γ-rays + UV: 7.00 ± 0.38 (median±σ). The differences between the groups are also reliable ($p<0.01$ against the Mann – Whitney U-test), excluding the "UV and γ-rays" pair ($p=0.69$). In the 10th month, the lens morphology and changes in its protein composition were studied. All the experimental groups showed morphological changes in the lens, but no changes were found that would be specific to any group. Though it had been shown earlier that the radiation cataract consists mainly in the formation of posterior cortical opacities, it was established in later research that the diffuse cataract is the most common in this case.

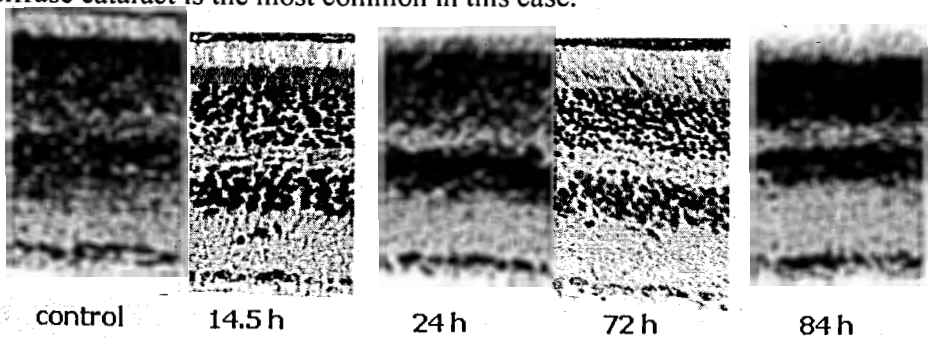

Fig. 11. Microphotos of histological cuts of a mouse retina before and after γ-irradiation.

To study the histological changes in the lens, semifine sections and a spread epithelium preparation were used. Epithelium microscopy was done using a Technival (Carl Zeiss Jena) microscope equipped with a Nikon CoolPix P5000 digital photocamera (Fig. 11). It should be noted that cortical parts of the lens were studied – the parts where opacities were mainly found. The general structure of the tissue, the mitotic index, and the presence of the following pathologic changes were examined: nuclei with vacuoles and macronuclei; cavities in the epithelium stratum; multilayer structures formed by transformed epithelial cells; desquamed cells; and cells with vacuoles in cytoplasm. A study of the lens epithelium also revealed an effect that is common to all exposures: a decrease in the density of cells. It agrees with the data showing that ionizing radiation, UV radiation, and aging decrease the density of lens epithelium cells. Thus, in the investigation of microscopic preparations, non-specific changes related to the aging of animals were found that are arranged in the order of increasing as follows: R, UV, gamma, gamma + UV. It should be noted that the lens opacity degree increased in the same order.

The lens proteome was studied using the differential electrophoresis technique. Lenses of animals in which the cataract matched the group median were used as samples; the opacity degree of the right and left lenses was considered to be equal. For an analysis, the following sample pairs were used: "R and gamma," "R and UV," "R and gamma + UV," "gamma and UV," and "gamma and gamma + UV." One of the samples in a pair was stained with the Su-3 fluorescent dye ($\lambda_{ex/em}$=532/580); the other – with Su-5 ($\lambda_{ex/em}$=633/680). After separation by equipment for two-dimensional electrophoresis (BioRad, the U.S.), the gel was scanned by the Typhoon 9410 (GE Healthcare) laser scanner. In the gel image, the proteins represented in both samples of a pair are painted yellow; different ones – green (Su-3) or red (Su-5). The images were analyzed with the DeCyder (GE Healthcare) program. All the stains in the electrophoretic patterns of the pairs "R and gamma," "R and UV," "R and gamma + UV," "gamma and UV," and "gamma and gamma + UV" – both in water-soluble and water-insoluble fraction of the proteins – turned out to be yellow. According to the differential electrophoresis principle, it means that these sample pairs do not differ in the protein composition. Thus, a long exposure to low UV doses, a γ-irradiation with a dose of 2 Gy, and their joint effect do not influence the protein composition of both the soluble and insoluble fractions of the mouse lens. Research on changes in the protein composition of the lens developing

with the organism aging and/or cataract formation clearly showed that protein molecules undergo post-translational modifications. It was expected that UV irradiation in the range of 280 – 390 nm should have a stronger damaging effect. But the integral method of differential electrophoresis showed that there is not any significant difference between aging, UV action, and radiation action. It can be attributed either to the actual absence of differences or to the sensitivity of fluorescent dyes being lower than that of staining with silver.

An idea was repeatedly expressed in literature that ionizing or UV radiation can be used to model senile cataract formation, but suggestions to the contrary were also made. In this work, a complex study of cataract development was performed for the first time based on using randomized experimental groups.

Thus, the results of this comparative research show that the aging process, UV and/or γ-irradiation result in indistinguishable changes in the lens at all levels of its organization: molecular, cellular, and organ ones.

Gel filtration and small-angle X-ray scattering studies of the α crystallin showed that irradiation by B^{11} nuclei does not result in any significant changes either in the size or shape of the molecule. Also, no protein subunit linkages were observed (electrophoresis in PAAG). No changes in the chaperone activity against the thermal denaturation of the β_L crystallin were also observed, but some decrease in the protein chaperone activity was observed against photo aggregation.

Irradiation with 500–MeV C^{12} nuclei of the α and β_L crystallin was performed twice, but no significant changes were observed.

Irradiation with Li nuclei did not affect the β_L crystallin stability against thermal denaturation. A study of the protein stability against photo aggregation under UV light showed that irradiation shortens the lag phase and accelerates aggregation. However, the dose dependence turned out to be essentially non-linear: the photo aggregation acceleration was maximal for a dose of 4 Gy, while a dose of 16 Gy did not lead to any deviation from the reference level. The electrophoresis data also showed no radiation-induced changes in the polypeptide composition of the samples. A study of fluorescence spectra showed that there are no evident changes in molecular spectra. A gel filtration study of the α crystallin showed that irradiation does not cause significant changes in the size of the molecule; also, no protein subunit linkages were observed (electrophoresis in PAAG). No changes in the chaperone activity against thermal denaturation of the β_L crystallin were

observed. But, like under irradiation by B^{11}, some decrease was observed in the chaperone activity of the protein against photo aggregation.

Thus, on the grounds of the obtained results, it is possible to conclude that high-energy nuclei (500 MeV) with a dose rate of 4 Gy/h do not affect crystallins, while nuclei with an energy of about 40 MeV with a dose rate of 4 Gy/min can damage both α and β_L crystallin molecules. The results, however, are rather contradictory and require further research.

2.3. *Computer molecular modeling of biophysical systems*

The research performed by the Computer Molecular Modeling Sector included molecular dynamics (MD) simulation of physical nanosystems and radiobiological objects in terms of mutated proteins and was based on modern high-performance computational methods and clusters. Molecular dynamics research has been performed in close collaboration with leading molecular simulation centers of Japan (RIKEN Genomic Science Center in Yokohama and Keio University) and England (Daresbury Laboratory).

MD simulation is one of the most powerful methods of studying properties of biological (protein) molecules. The calculation of relaxed conformational states for mutated proteins on the basis of traditional computational approaches may take years even for a single structure evaluation. Structural and conformational changes in physical and biological systems are mostly correlated with the influence of physical, chemical or environmental factors. In biological objects like DNA or proteins, the influence of radiation and high-energy proton and ion beams results in mutational changes in the DNA structure and subsequent conformational reconstruction and structural changes in mutated proteins. It is well known that the conformational shape behavior (i.e. folding) of biological (protein) molecules directly defines their specific functional behavior. The observation and quantitative estimation of the effects of mutation exchanges in protein structures, where the current research is aimed, presents a fundamental problem of great importance. In modern computational chemistry and nanobiotechnology, the efficient MD algorithms are well developed; they allow reconstructing the properties of molecular systems with a high accuracy or predicting their nontrivial dynamics and new phenomena. The basic and well-known difficulty that obstructs the efficient use of MD for studying extended molecules like proteins consists in the huge system size (from tens up to million atoms) and the scale of the time necessary for the computation of the dynamics of nanosystems and

conformation structures of proteins (from femto- up to pico- and nanoseconds and greater time scales). Thus, without modern powerful computational facilities and resources, newest processors and platforms, and their adequate adaptation to MD modeling, the problem cannot be solved successfully. A number of research and educational projects that are realized within MD simulation approach are outlined below.

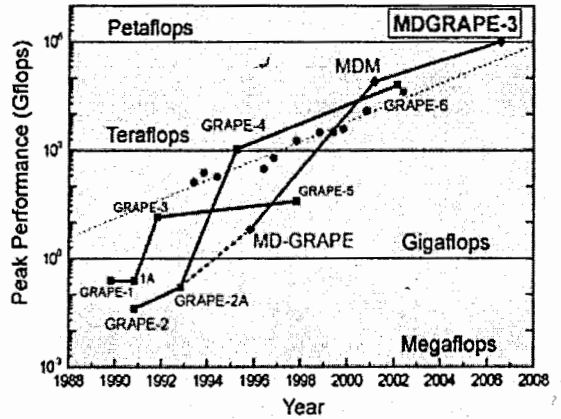

Fig. 12. A peak performance of the different versions of GRAPE systems.

MD simulation was performed in a number of papers; code for computational chemistry and nanotechnology problems was developed and optimized in different network communication architectures at JINR's Central Information and Computing Complex (CICC). These reports compare the performance of the DL_POLY general-purpose molecular dynamics simulation package on the LIT JINR computing cluster CICC in various communication systems. The comparison of the DL_POLY codes involved two cluster architectures using the Gigabit Ethernet and InfiniBand technologies, respectively. The code performance tests included some comparison of the CICC cluster with the special-purpose MDGRAPE-3 computer developed at RIKEN for high-speed MD modeling without the cutoff radius of long-range forces (Fig. 12).

MD simulations of the visual pigment rhodopsin with the E181K mutation, which is associated with retinitis pigmentosa, are performed in Collaboration between JINR and N.M. Emanuel Institute of Biochemical Physics (RAS). Autosomal dominant retinitis pigmentosa leads to the photoreceptor cell death and retina degeneration. Approximately 25% of this pathology is associated with the rhodopsin gene mutation RP4(RHO)/Rhodopsin(3q). The amino acid substitution in the chromophore

center during rhodopsin biosynthesis leads to the most distinctive clinical pathology of this inherited disease. The consequence of mutations like these is protein misfolding. As a result, formation of a stable Schiff base linkage between the 11-cis-retinal chromophore and amino acid residue Lys296 is impossible. Using molecular simulation technique, the process of the 11-*cis*-retinal chromophore embedding into the chromophore center of an opsin mutant form has been investigated. The comparative analysis of amino acid residues arrangement in the opsin chromophore center and its interaction with 11-*cis*-retinal as in the wild (native) and in mutant opsins has been carried out. It was shown that there is no normal embedding of 11-*cis*-retinal into the chromophore center of an opsin mutant form. As a result, the impairment of the conformation state of the opsin molecule takes place both in the chromophore center and in the cytoplasmic domain. A stable covalent linkage of 11-*cis*-retinal with the protein part of the rhodopsin molecule is not formed; also, the active site in the cytoplasmic domain of the protein that is responsible for binding of the G-protein (so-called transducin) is not completely blocked. Based on the molecular simulation data, the problem related to retinitis pigmentosa pathogenesis is discussed (Fig. 13).

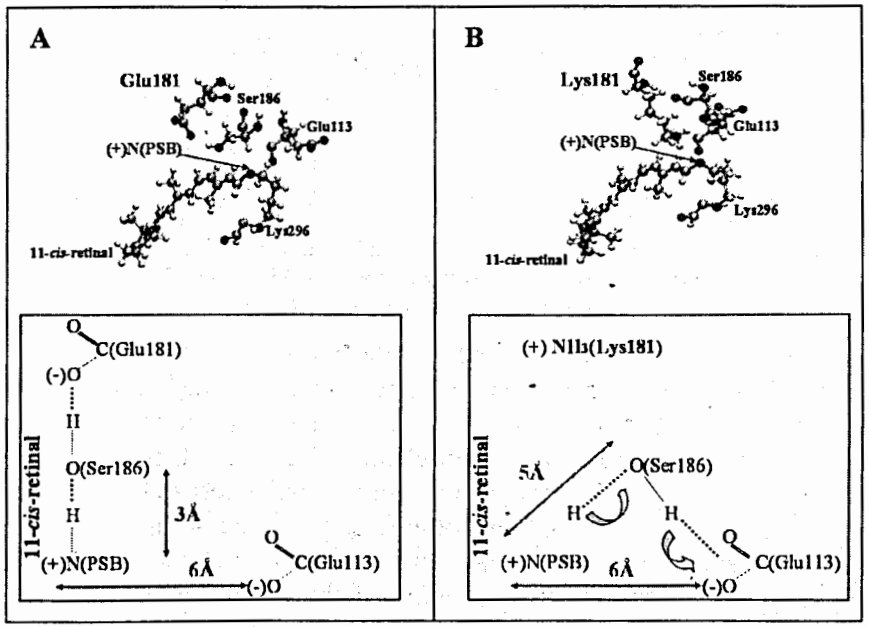

Fig. 13. MD analysis of the native (left) and mutant E181K forms of the rhodopsin protein.

A comparative analysis of 3D simulation of different allele forms of the human kinase CDK2 has been performed. The crystal structures of the human CDK2/cyclin A complex has been modeled. The structure was modeled of the wild type and a mutant allele with a single substitution of glycine with serine in the position 16 (G16S) in the conservative G-rich loop. It was shown that this substitution causes a serious modification in the protein structure. In yeast, such changes of the CDC28 homologous kinase have serious pleiotropic biological effects. To investigate the significance of the observed structural modifications, the structure was studied of another mutant allele – R274Q – which has no biological effects in yeast at a permissive temperature. The comparison of simulated CDK2 structures of three alleles shows that the root mean square deviation of the kinase and kinase+ cyclin does not change in the last allele of the kinase, although the structures of the T- and G-loops were modified. These results confirm the correlation between the observed changes in the kinase structure and the biological effect (Fig. 14).

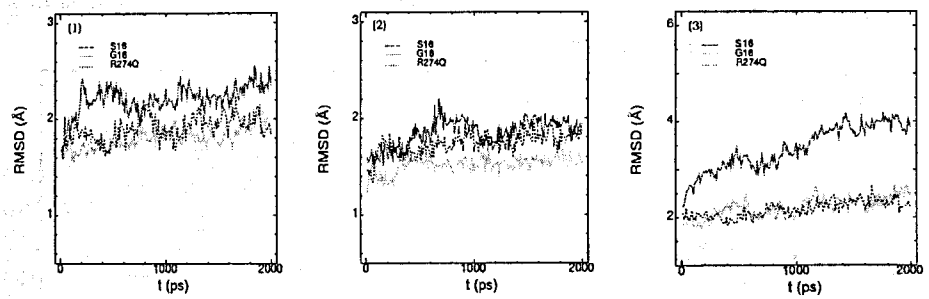

Fig. 14. Time dependence of configurations for different forms of the CDK2 kinase: the wild-type (G16 R274) and mutant forms (G16S and R274Q) kinase (1), cyclin (2), kinase+cyclin (3).

MD simulation measurements of the partial molar volume limit of mono-carboxylic acids in benzene were performed in collaboration between JINR, the Skobeltsyn Institute of Nuclear Physics (Lomonosov Moscow State University), and Taras Shevchenko National University (Kyiv, Ukraine). The limit thermodynamic molar characteristics of solutions contain information about the hypothetic state of the solute molecules at infinite dissolution. Thus, the limit partial volume reflects the compressibility of the structure packing of the solute molecule under the action of the solvent. Here, this volume is determined by means of molecular dynamics simulation of limit solutions. For this purpose, the integral analysis of the found radial distribution functions is used. The

method is applied to study solutions of mono-carboxylic acids (non-saturated oleic and saturated stearic and myristic acids) in benzene, which are widely used in practice for the stabilization of magnetic fluids (fine liquid dispersions of magnetic nanoparticles coated with surfactants). The found volume values are in agreement with experimental data of vibration densitometry and small-angle neutron scattering research. The structure organization of the solvent at the molecule interface is compared for the acids with respect to their different properties of stabilizing magnetic fluids.

2.4. Radiation research

In 2003–2009, LRB specialists participated in the design of radiation protection systems of nuclear physics facilities. Much work was done for the project of the Slovak Cyclotron Complex (Bratislava) taking into account all available physical and medical technologies. The following aspects of radiation safety were considered: criteria and measures concerning radiation safety, radiation sources, biological protection, the skyshine problem, radiation monitoring arrangements, radioactive waste treatment, possible radiation accidents, etc.

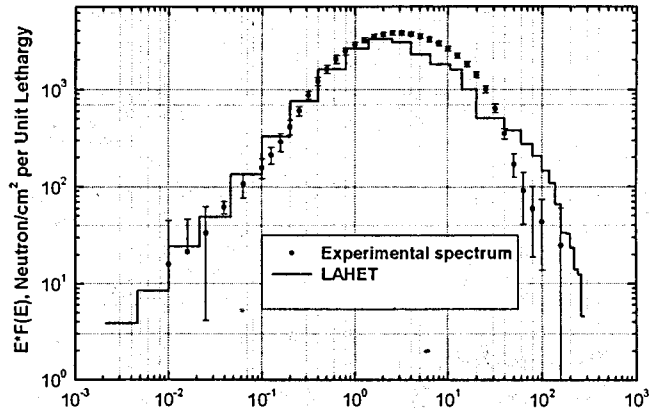

Fig. 15. A comparison of calculation by the LAHET code with the experimental spectrum of neutrons emitted at an angle of 105° from a thick Pb target irradiated with a 650-Mev proton beam.

Another major project was focused on the creation of a subcritical assembly driven by a proton beam of the LNP Phasotron (the SAD project). To obtain the initial data, some experiments were performed to measure of double differential hadron yield from a thick plumb target irradiated with

650-MeV protons. The experimental data were compared with the results of MC calculations done using the MCNP4B+LAHET and MCNPX programs (Fig. 15). Measured were the spatial distribution of the neutron dose rate around the facility location and the induced activity of the Phasotron bank soil. Within the framework of the project, the assembly core and magnet hall shieldings were calculated; radiation zones were determined; induced radioactivity of the equipment, air, and soil was estimated; and a forecast of radiation conditions around the SAD building was made.

The following work was being done: the prediction of radiation conditions at the IREN facility and its shielding calculation; design of the shielding and modeling the parameters of the DViN-1 and DViN-2 facilities for detecting explosives and drugs; calculation of the background radiation of the n–n scattering facility, etc.

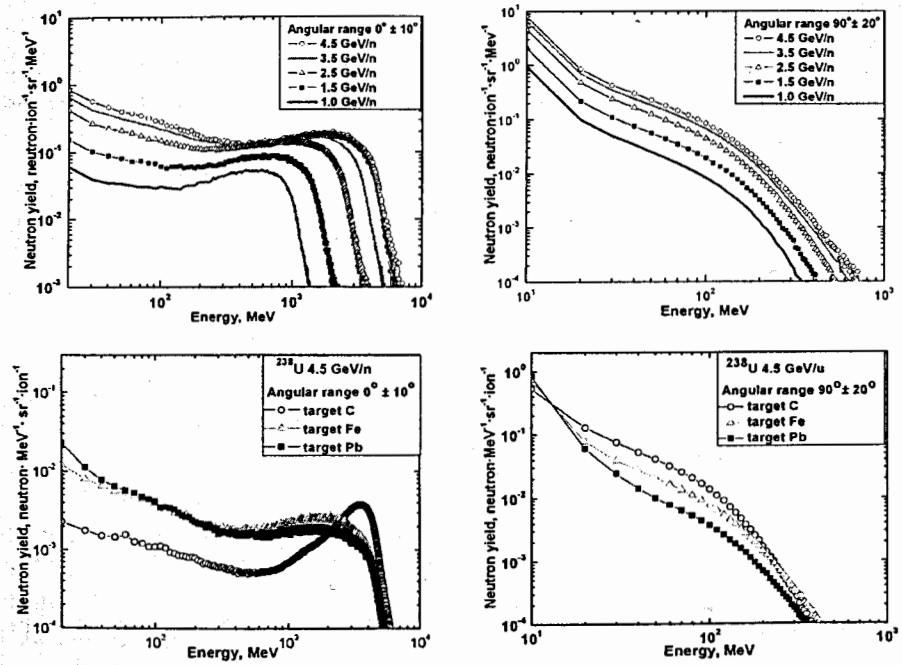

Fig. 16. Double differential neutron yields in the interaction of uranium nuclei of different energies with a thick target of different materials.

In 2008, calculation of the shielding and radiation performances of the NICA accelerator complex was started. The shielding calculation criteria were determined. A collation of experimental data and a number of

MC-based programs of ion transport in matter was made. Mathematical models of the radiation sources of the NICA complex were developed; shielding design variants were suggested; and calculations were performed of the spatial distribution of skyshine neutrons produced by separate sources and by the whole complex for its different configurations and parameters. The modeling of the induced radioactivity accumulation in equipment elements was begun. Fig. 16 shows the results of the GEANT4 code calculations of double differential neutron yields in the interaction of uranium nuclei of different energies with a thick target of different materials.

Throughout the whole reporting period, in cooperation with the Institute of Space Research and the Laboratory of Neutron Physics, work was continued under the program of research of planet surfaces with nuclear physics methods. LRB specialists participate in the development and design studies, calibration, and computer modeling of related instruments. The most significant result of this cooperation is exemplified by the successful work of the Russian HEND detector of albedo neutrons on board the U.S. spacecraft *Odyssey* on the orbit of Mars. On the grounds of its readings, the Martian surface was mapped, and significant amounts of water were reliably discovered not only on the polar caps, but also in the middle latitudes. The Russian LEND neutron detector on board the U.S. spacecraft placed into the Moon orbit in the summer of 2009 is another successfully working device. Its readings allowed mapping the hydrogen distribution over the Moon surface. Much work was done concerning the development, testing, and calibration the time spectrometer of albedo neutrons for NASA's Mars rover with a neutron generator (the Russian project DAN), and the development of a neutron and gamma spectrometer for the Russian "Phobos Soil" mission.

In the reporting period, radiobiological experiments were regularly carried out at charged particle beams of the Phasotron (protons), U-400M cyclotron (^{7}Li, ^{11}B, and ^{14}N nuclei), and Nuclotron (protons, ^{4}He, ^{12}C, and ^{24}Mg). At the U-400M cyclotron, experiments were performed using the "Genom" automated irradiation device, which is now reconstructed in cooperation with FLNR.

Much attention was paid to the development of the technique of neutron spectrometry in scattered radiation fields behind accelerator shielding and in the environment. Using the MCNP code, a detailed calculation of the response functions of a multi-sphere spectrometer for neutrons with energies up to 20 MeV was performed. A heterogeneous

sphere with a plumb insert was produced to make the spectrometer more informative regarding high-energy neutron range. In 2009, an autonomous portable netbook-based spectrometer was developed and produced for neutron measurements in the environment.

Research was continued on the performances of different radiation detectors. Calculations were performed of the X-ray detection by silicon and scintillation detectors. Measured were the sensitivity of the PADC, PETF, and CR-39 track detectors and the dependence of the diameter of tracks in CR-39 on LET for ^{12}C, ^{24}Mg, ^{40}Ar, and ^{56}Fe nuclei with energies up to 0.5 GeV/nucleon. The results were processed of a verification of different passive detectors used in space dosimetry, which was performed at ^{4}He, ^{12}C, ^{28}Si, and ^{56}Fe beams with energies of 150, 400, 490, and 500 MeV, respectively (ICCHIBAN, Japan). Studies were continued of the sensitivity functions of the PADC and PETF track detectors at beams of JINR's accelerators. A methodology was developed of the correction of the readings of the individual albedo neutron dosimeters and neutron dosimeters based on SNM-14 counter witin a moderator. The methodology was developed from the systematization of neutron spectra in the radiation fields of facilities of JINR and a number of foreign centers. An algorithm was suggested of the calculation of a ridge filter to form a carbon nuclei beam for the target therapy of tumors.

Since 2008, under the Intergovernmental Scientific Agreement between Russia and India, experiments have been carried out within the framework of Project A-2.53 PUC-12/JC-XII at the medical beam of the LNP Phasotron to study of characteristics of designed in India new nanocrystalline thermoluminescent detectors; also, properties of protective materials have been investigated using isotope neutron sources.

3. Scientific research programme for 2010

The central problem of fundamental radiation genetic research is the clarification of the molecular mechanisms of mutagenic effects induced by different types of ionizing radiation in cells with various levels of genetic organization. Heavy charged particles are a powerful tool for such studies. DNA damage induced by heavy ions is essentially different than that induced by γ-rays. It is established that clustered DNA lesions are formed under heavy-ion irradiation. The repair of such lesions is strongly repressed. These circumstances determine different radiation effects induced by accelerated charged particles and sparsely ionizing radiation.

Research and development will include:

- Acquisition of new data on molecular DNA damage in human cells under heavy ion irradiation;
- Study of the formation of structure lesions in the chromosome apparatus under low doses of radiation with different linear energy transfer;
- Acquisition of new data on the genetic control of the induced mutation process in cells with different levels of the genome organization;
- Comparative evaluation of the influence of therapeutic proton and carbon beams on human cells based on cytogenetic disorders in peripheral blood lymphocytes;
- Study of the effects of accelerated heavy charged particles on eye structures (the lens and retina);
- Molecular dynamics simulation of radiation-induced damage and mutations in biological structures;
- Mathematical modelling of induced mutagenesis in cells with different genotype;
- Calculation of radiation protection measures for new nuclear physics facilities, evaluation of their radiation situation, and development of radiation safety systems for them;

As the results the following items will performed:

- Continuation of studying regularities in the induction of different types of DNA lesions, apoptosis, and repair in human lymphocytes in different phases of the cell cycle under ionizing radiations with different physical properties in the presence of modifiers;
- Study of the combined effect of γ-radiation and lipid *A* obtained from *Escherichia coli* on phagocytosis, lysozyme, and peroxidase activities of human peripheral blood lymphocytes
- Acquisition of data on the influence of a disorder in the mitochondrial genome on the lethal and mutagenic effects of ionizing and non-ionizing radiation;
- Acquisition of data on the role of the active forms of oxygen and intracellular signal systems in the formation of the dose dependence of the chromosome aberration induction in mammalian and human cells by low doses of radiation;
- Acquisition of data on the regularities of cataract induction in mice by 100–200-MeV protons;
- Mathematical modeling of the mutagenic effect of ionizing radiation with different linear energy transfer on bacterial cells;

- Dosimetric and physical support of radiobiological experiments at the VBLHEP Nuclotron, FLNR cyclotron U400M and the medical beam of the DLNP Phasotron;
- Molecular dynamics simulation of structures of biologically important macromolecules;
- Prediction of the radiation situation at JINR's new nuclear physics facilities and aboard spacecraft.

4. Scientific meetings and educational activity

On 15 December 2008, a general meeting of the Section of Biological Sciences, Russian Academy of Sciences (SBS RAS), was held under the chairmanship of the RAS Vice-President Acad. A.I. Grigoryev. It was concerned with a long-term forecast of the development of a number of fields in fundamental biology. Among the issues considered at the meeting was a proposal of the scientific and methodological supervision of the Laboratory of Radiation Biology (LRB), JINR, by the SBS RAS. The LRB's main activity is research on the regularities and mechanisms of the biological action of ionizing radiations with different physical characteristics. The LRB Director Prof. E.A. Krasavin presented a report on the LRB's research and main scientific results. The meeting unanimously supported a proposal by the SBS RAS Bureau and resolved to provide the scientific and methodological supervision of the LRB by the SBS RAS (resolution No. 5 of 15 December 2008).

The report reviewed the results of the radiobiological research which has been performed for many years at JINR accelerators and JINR's capabilities of solving fundamental and practical problems of modern biology and medicine. Half a century ago, JINR made an important contribution to the success of the first manned space flights as there was an essential issue of estimating the damaging effect of high-energy protons on the human organism. At the synchrocyclotron – JINR's proton accelerator – large-scale radiobiological research was carried out which allowed taking the necessary measures to lower the radiation risk to the crew members of orbital flights. In the near future, regarding the flights beyond the Earth's magnetosphere – like the Moon exploration or manned flights to the Mars – there will be an extremely urgent problem of the biological action of high-energy heavy charged particles (HCP) emitted from the depth of the galaxy. In these conditions, the spacecraft crew members will be chronically exposed to accelerated heavy ions of wide energy and charge spectra, which

can lead to different kinds of adverse consequences for the organism. They include an increased risk of cancer development, gene and structure mutations, visual apparatus disorders (development of a cataract and retina lesions), and damage to the central nervous system structures. The specifics of the disorders in a number of physiological mechanisms caused by organism exposure to the HCP are associated with the following special feature of the high-energy heavy ion energy transfer to the biological structures: much energy is released in a small volume of matter. JINR's multi-charged ion accelerators allow carrying out research aimed at modeling the biological action of the heavy nuclei of the galactic cosmic radiation. The report presented the results of the research on the mechanisms of the lethal and mutagenic affect of multi-charged ions on cells of different organisms, molecular mechanisms of cataract development under exposure to radiation with a wide range of the linear energy transfer, HCP damaging effect on the retina and central nervous system tissues, and blastomogenic effects of corpuscular radiation.

Thus, in the modern period, JINR's unique research facilities will be remarkably valuable for solving a number of urgent problems in medicine and biology which are not only fundamental but also very important practically.

In June 2006, the 4th International Workshop on Space Radiation Research and 17th Annual NASA Space Radiation Health Investigators' Workshop was held in Moscow and St. Petersburg. The major role in the organization of these meetings belonged to the Laboratory of Radiation Biology (JINR) and the Institute for Biomedical Problems of the Russian Academy of Sciences (RAS). Modern problems of classical and space radiobiology, space radiation protection, dissymmetry, etc. were discussed at the workshops. Special attention was given to the Moon exploration program, Mars manned flight program, as well as to possible uses of the obtained data in applied medicine, biology, and radiation protection. The workshops were attended by more than 100 scientists from Russia, USA, Germany, Italy, Japan and JINR took part in it.

In January 2007, the Russian Academy of Sciences (RAS), the RAS Division of Biological Sciences of the Russian Academy of Sciences, the Bach Institute of Biochemistry of RAS, the Russian State Scientific Centre "Institute of Biomedical Problems" of RAS, together with the Bunatian Institute of Biochemistry of the National Academy of Sciences of the Republic of Armenia, Yerevan State University, and JINR held the III

International Symposium "Problems of Biochemistry, Radiation and Space Biology" dedicated to the centenary of the birth of Academician Norair Sissakian.

The International Symposium "Modern spectroscopy methods in studying structure and function of biopolymers in biology and medicine" which was organized by the RAS Council on Biophysics, Laboratory of Radiation Biology (JINR), and M.V. Lomonosov Moscow State University, took place in June 2007 at the International Conference Hall in Dubna. The symposium was supported by the International Union for Pure and Applied Biophysics (IUPAB). Modern methods of spectroscopy are very efficient in biopolymer research and have a great advantage of being non-invasive ones. They are successfully used for bioindication of different diseases since they provide an opportunity to detect the primary stages of various pathogenic changes. Biomedical spectroscopy is boundary area in biophysics where a great number of new results have been obtained in recent years. About 80 scientists from JINR, Armenia, Azerbaijan, Belarus, Bulgaria, Canada, Denmark, France, Germany, Russia, Switzerland, and the U.S. participated in the symposium. The symposium programme included 30 plenary reports on fundamentals basis of spectral methods and the results of their application in biomedicine. Special attention was given to the analysis of the primary processes of the optical and ionizing radiation effects on biopolymers, as well as infrared spectroscopy-based, radiobiological, polarized fluorescence-based, acoustic, gamma-ray and optical spectroscopy-based, and others techniques using in biomedicine.

In October 2007, the International Workshop of Multilateral Medical Operations Panel (MMOP) and Multilateral Radiation Health Working Group (MRHWG) was held in Dubna under the direction of LRB.

The 1st, 2nd, and 3rd International workshops "Molecular Simulation Studies in Material and Biological Sciences" (MSSMBS 2004, 2006, and 2008) were organized at JINR. Contributions were mostly by leading molecular simulation centers of Japan and Russia including European research groups. These workshops were attended by scientists from research centers and universities of Japan and Russia (the Institute of Bioorganic Chemistry, Institute of Biochemical Physics, Institute of Mathematical Problems of Biology, MSU, etc) as well as from the Laboratory of Radiation Biology, Flerov Laboratory of Nuclear Physics, and Laboratory of International Technologies. The workshop programs reflected the current status and prospects of computer molecular simulation in material and life sciences and covered the following topics: protein modeling, drug design, simulation of liquids and polymer systems, simulation of radiation-induced damages and mutations, quantum biophysics, and parallel computing for chemical physics and biomolecular studies.

During 2009 LRB scientists participated in more than 15 conferences in Russia and more than 6 international conferences in Europe and Asia.

The education process continued at the Department of Biophysics, Dubna University. The Department's total enrolment is 88 in the specialty "Human and Environmental Radiation Protection" and two postgraduate students in the specialty "Radiobiology". 15 students were admitted in 2009 to the Department. The fifth graduation (20 students) took place in 2009.

The education activity of Computer Molecular Modeling Sector (CMM) staff included the supervision of diploma projects and teaching a course of molecular dynamics to students of Dubna University. A number of diploma projects on different aspects of homology modeling and molecular dynamics of nanosytems and proteins were successfully completed and defended. The courses have been offered at the Department of Biophysics and Department of Chemistry, Geochemistry, and Cosmic Chemistry. In 2007 the CMM head Dr. Kh.T. Kholmurodov gave lectures at the Physics Department of the College of Science, Sultan Qaboos University (Oman). A number of reviews and reports were made concerning PhD theses prepared by students of Egypt (Cairo University), Uzbekistan (Institute of Nuclear Physics), and Tajikistan (Tajik National University). In 2009, Dr. Kh.T. Kholmurodov was appointed a Visiting Professor at the Faculty of Science and Technology of Keio University – one of the top private universities in Japan.

5. Administration activity

Staff The total staff of the LRB is 85, including the directorate staff of 15.

Finances The funding of radiation and radiobiological research in 2009 is shown in Table 1.

Table 1. LRB financing

Area	Financing plan (k$ USA)						
	2004	2005	2006	2007	2008	2009	2010
08-9-1015-96/2008	265.8	275.1	331.0	393.9	469.6		
04-9-1077-09/2011						674.0	693.7
Infrastructure	87.2	71.3	74.0	141.4	121.4	179.7	164.0
Total	**363.0**	**346.4**	**405.0**	**535.3**	**591.0**	**853.7**	**857.7**